ISSN 1674-1056
http://cpb.iphy.ac.cn
http://iopscience.iop.org/cpb
中国物理 B
Chinese Physics
中国物理
Chinese Physics B

Boundary states for entanglement robustness under dephasing and bit flip channels

Hong-Mei Li(李红梅), Miao-Di Guo(郭苗迪), Rui Zhang(张锐), Xue-Mei Su(苏雪梅)
Citation: Chin. Phys. B . 2019, 28(10): 100302 . **doi:** 10.1088/1674-1056/ab3e67
Journal homepage: http://cpb.iphy.ac.cn; http://iopscience.iop.org/cpb

What follows is a list of articles you may be interested in

Dipole-dipole interactions enhance non-Markovianity and protect information against dissipation

Munsif Jan, Xiao-Ye Xu(许小冶), Qin-Qin Wang(王琴琴), Zhe Chen(陈哲), Yong-Jian Han(韩永建), Chuan-Feng Li(李传锋), Guang-Can Guo(郭光灿)
Chin. Phys. B . 2019, 28(9): 090303 . **doi:** 10.1088/1674-1056/ab37f2

Geometrical quantum discord and negativity of two separable and mixed qubits

Tang-Kun Liu(刘堂昆), Fei Liu(刘飞), Chuan-Jia Shan(单传家), Ji-Bing Liu(刘继兵)
Chin. Phys. B . 2019, 28(9): 090304 . **doi:** 10.1088/1674-1056/ab37f6

Dissipative generation for steady-state entanglement of two transmons in circuit QED

Shuang He(何爽), Dan Liu(刘丹), Ming-Hao Li(李明浩)
Chin. Phys. B . 2019, 28(8): 080303 . **doi:** 10.1088/1674-1056/28/8/080303

Tetrapartite entanglement measures of W-class in noninertial frames

Ariadna J. Torres-Arenas, Edgar O. López-Zúñiga, J. Antonio Saldaña-Herrera, Qian Dong, Guo-Hua Sun, Shi-Hai Dong
Chin. Phys. B . 2019, 28(7): 070301 . **doi:** 10.1088/1674-1056/28/7/070301

Atom interferometers with weak-measurement path detectors and their quantum mechanical analysis

Zhi-Yuan Li(李志远)
Chin. Phys. B . 2019, 28(6): 060301 . **doi:** 10.1088/1674-1056/28/6/060301

Boundary states for entanglement robustness under dephasing and bit flip channels*

Hong-Mei Li(李红梅), Miao-Di Guo(郭苗迪), Rui Zhang(张锐), and Xue-Mei Su(苏雪梅)†

College of Physics, Jilin University, Changchun 130012, *China*

(Received 16 May 2019; revised manuscript received 13 August 2019; published online 25 September 2019)

We investigate the robustness of entanglement for a multiqubit system under dephasing and bit flip channels. We exhibit the difference between the entanglement evolution of the two forms of special states, which are locally unitarily equivalent to each other and therefore possess precisely the same entanglement properties, and demonstrate that the difference increases with the number of qubits n. Moreover, those two forms of states are either the most robust genuine entangled states or the most fragile ones, which confirm that local unitary (LU) operations can greatly enhance the entanglement robustness of n-qubit states.

Keywords: entanglement, decoherence, robustness, local unitary equivalence

PACS: 03.65.Yz, 03.65.Ta, 03.65.Ud **DOI:** 10.1088/1674-1056/ab3e67

1. Introduction

Quantum entanglement is one of the most intriguing features of quantum mechanics.[1,2] It is a major resource for quantum information processing (QIP), such as quantum computation,[3,4] quantum teleportation,[5,6] quantum key distribution,[7–9] and distributed quantum learning.[10] Recently, much attention has been paid to the unavoidable degradation of entanglement due to decoherence in realistic environment.[11–13] The entanglement of a bipartite quantum system can decay to zero abruptly under the effect of local environment, which is a well-known decoherence phenomena named as entanglement sudden death (ESD).[14–17] It was shown that the ESD is related to the type of initial state.[18,19]

There are many excellent papers have been devoted to the study of the robustness of various bipartite[20,21] and multipartite entangled states under different decoherence models.[22–26] It is possible to calculate the exact value of the geometric measure of entanglement for special states under collective dephasing.[22] In addition, the robustness of entanglement for some highly entangled multiqubit pure states against various decoherence is obtained.[23] To make a thorough understanding about the robustness of a specific state, it is useful to compare it with random states.[24] For a two-qubit system under decoherence,[20] we find that the Bell-like states are always the most robust ones; for the three-qubit system,[27] we investigated the entanglement robustness under amplitude damping, dephasing and bit flip channels, respectively, and found the most robust genuine tripartite entangled states and the most fragile ones.

The entanglement robustness for the case of n-qubit states has been extensively analyzed.[23,28,29] By studying the disentanglement dynamics of the generalized N-qubit GHZ states under the amplitude-damping channel, some authors affirm that the entanglement robustness can be enhanced by local unitary (LU) operations though the amount of entanglement itself cannot.[28] However, they did not discuss to what extent the robustness of entanglement can be enhanced. It is of theoretical interest and has potential application in accomplishing some quantum task.

In this paper, we investigate the robustness of n-qubit states under the dephasing and the bit flip channels. Negativity corresponding to the partitions "the first qubit *versus* the rest" will be used as the entanglement quantifier. We show how the entanglement evolution of two forms of special states, which are local-unitarily equivalent to each other and therefore possess precisely the same amount and type of entanglement in absence of decoherence, is influenced by the number of qubits n. We also find that the two forms of states exhibit the most significant different robustness by comparing with random states, which further confirm the important fact that the entanglement robustness of an n-qubit system can be greatly enhanced by LU operations.

The paper is organized as follows. In Section 2 we briefly introduce our environment models and entanglement measure for some special multiqubit systems. In Sections 3 and 4 we investigate the robustness of entanglement under the dephasing and the bit flip channels, respectively. Finally, we summarize our conclusions in Section 5.

*Project supported by the National Key Research and Development Program of China (Grant No. 2016YFE0200700) and the National Natural Science Foundation of China (Grant Nos. 61627820 and 61934003).

†Corresponding author. E-mail: suxm@jlu.edu.cn

© 2019 Chinese Physical Society and IOP Publishing Ltd

2. Noise models and entanglement measure

We consider a multi-qubit system interacting with dephasing and bit flip channels, respectively. We assume that each qubit in the composite system is coupled to its own noisy environment and there is no interaction between qubits. That is, all qubits are affected by the same decoherence process. The dynamics of a single qubit is governed by a master equation that gives rise to a completely positive trace-preserving map (or channel) ε describing the corresponding evolution:[23] $\rho_i(t) = \varepsilon(t)\rho_i(0)$. In the Born–Markovian approximation, the channel can be described by a set of Kraus operators[23,30,31] as

$$\varepsilon(\rho_i(0)) = \sum_{j=1}^{M} E_{ji}(t)\rho_i(0)E_{ji}^{\dagger}(t), \tag{1}$$

where $E_j(t)$ $(j = 1,\ldots,M)$ are the Kraus operators needed to completely characterize the channel which fulfill the normalization condition $\sum_j E_j^{\dagger}(t)E_j(t) = I$.

We start by discussing the dephasing channel, which can be also regarded as a phase flip channel. It describes the loss of quantum coherence without any exchange of energy. The Kraus operators for the dephasing channel are

$$E_0 = \begin{pmatrix} 1 & 0 \\ 0 & \sqrt{1-p_{\rm d}} \end{pmatrix}, \quad E_1 = \begin{pmatrix} 0 & 0 \\ 0 & \sqrt{p_{\rm d}} \end{pmatrix}. \tag{2}$$

Another type of environment to be dealt with is bit flip channel. The corresponding Kraus operators can be given by

$$E_0 = \sqrt{1-\frac{p_{\rm bf}}{2}}\begin{pmatrix} 1 & 0 \\ 0 & 1 \end{pmatrix}, \quad E_1 = \sqrt{\frac{p_{\rm bf}}{2}}\begin{pmatrix} 0 & 1 \\ 1 & 0 \end{pmatrix}. \tag{3}$$

The parameter $p_{\rm d}, p_{\rm bf}$ in channels (2) and (3) can also be interpreted as the degree of decoherence of an individual particle in multiqubit system with $p_{\rm d}, p_{\rm bf} \in [0,1]$, where $p_{\rm d}, p_{\rm bf} = 0$ means no decoherence and $p_{\rm d}, p_{\rm bf} = 1$ complete decoherence. The factor of 2 in Eq. (3) guarantees that at $p_{\rm bf} = 1$ the ignorance about the occurrence of an error is maximal, and as a consequence, the information about the state is minimal.[30]

To examine the bipartite entanglement dynamics for n-qubit states, we use negativity $\mathcal{N}(\rho)$[32–34] as the measure of entanglement between the first qubit q_1 and the rest ones Q_{n-1} (hereafter denoted by $q_1|Q_{n-1}$). Negativity is extensively used in study of the multipartite entanglement dynamics, though it cannot detect the positive partial transpose (PPT) entangled states. Based on the trace norm $\|\rho^{\rm T_A}\|_1$ of the partially transposed density matrix $\rho^{\rm T_A}$ of a mixed state ρ, the entanglement can be written as[34,35]

$$\mathcal{N}(\rho) = \|\rho^{\rm T_A}\|_1 - 1. \tag{4}$$

The trace norm of any Hermitian operator A is $\|A\|_1 \equiv {\rm tr}\sqrt{A^{\dagger}A}$, which is equal to the sum of the absolute values of the eigenvalues of A. The partial transpose density matrix has negative eigenvalues $\mu_i < 0$ and positive eigenvalues $\mu_j > 0$, it satisfies ${\rm tr}[\rho^{\rm T_A}] = \sum_i \mu_i + \sum_j \mu_j = 1$, thus its trace norm reads in general $\|\rho^{\rm T_A}\|_1 = |\sum_i \mu_i| + \sum_j \mu_j = 1 + 2|\sum_i \mu_i| \equiv 1 + \mathcal{N}(\rho)$. Therefore, the negativity $\mathcal{N}(\rho)$ is defined as twice the absolute value of the sum of the negative eigenvalues of $\rho^{\rm T_A}$.

3. Robustness of entanglement under dephasing channel

3.1. Evolution of special states under dephasing channel

The dephasing channel reflects the decay of non-diagonal elements of density matrix with time. In this channel, we focus first on the n-qubit system in the form of pure states

$$|\Psi^n\rangle = \frac{1}{\sqrt{2^{n-2}}}\Big(\cos\theta|0\rangle \otimes \sum_{P_i}\widehat{P}_i|i_2,i_3,\ldots,i_n\rangle + {\rm i}\sin\theta|1\rangle \otimes \sum_{P_j}\widehat{P}_j|j_2,j_3,\ldots,j_n\rangle\Big), \tag{5}$$

where $\theta \in [0,\pi/2]$. $i_k, j_k = 0,1$ and $k = 2,3,\ldots,n$ with odd numbers of $\{i_k\}$ and even numbers of $\{j_k\}$ taking 1, respectively. $\widehat{P}$ means all possible permutations of $\{i_k\}$ and $\{j_k\}$. The initial entanglement of the above states (5) can be simply derived as $\mathcal{N}_0 = \sin 2\theta$.

In the following, we take the example of a four-qubit system in the pure state $|\Psi^4\rangle$ to calculate its negativity under the dephasing channel. We note that the negativity of the states (5) with $n = 4$ is determined by the partial transposed density matrix $\rho_{\Psi^4}^{\rm T_A}(t)$. The nonzero diagonal matrix elements of $\rho_{\Psi^4}^{\rm T_A}(t)$ are given by

$$\rho_{mm}(t) = \begin{cases} \dfrac{\cos^2\theta}{4}, & \text{with } m = 2,3,5,8; \\ \dfrac{\sin^2\theta}{4}, & \text{with } m = 9,12,14,15; \end{cases} \tag{6}$$

and the nonzero off-diagonal terms are given by

$$\rho_{mn}(t) = \begin{cases} \dfrac{\cos^2\theta}{4}s, & \text{with } m,n = 2,3,5,8, \text{and } m \neq n; \\ \dfrac{\sin^2\theta}{4}s, & \text{with } m,n = 9,12,14,15, \text{and } m \neq n; \end{cases} \tag{7}$$

$$\rho_{mn}(t) = \rho_{nm}^{*}(t) = {\rm i}\frac{\sin\theta\cos\theta}{4}s, \tag{8}$$

with $m = 1,4,6,7$, $n = 10,11,13,16$, and $n \neq 17-m$; and

$$\rho_{mn}(t) = \rho_{nm}^{*}(t) = {\rm i}\frac{\sin\theta\cos\theta}{4}s^2, \tag{9}$$

with $m = 1,4,6,7$, $n = 17-m$. Hereafter, $s \equiv 1-p_{\rm d}$ (or $p_{\rm bf}$) in the partially transposed density matrix.

The negativity corresponding to the bipartition $q_1|Q_{n-1}$ for the state $|\Psi^4\rangle$ can be readily calculated as

$$\mathcal{N}^{(4)} = \frac{1}{2}(1-p_{\rm d})(2+p_{\rm d})\mathcal{N}_0. \tag{10}$$

Similarly, the negativities for the states $|\Psi^n\rangle$ with $n = 2,3,5,6$, and 7 are given by

$$\mathcal{N}^{(2)} = (1-p_{\rm d})\mathcal{N}_0,$$

$$\begin{aligned}\mathcal{N}^{(3)} &= \mathcal{N}^{(2)}, \mathcal{N}^{(5)} = \mathcal{N}^{(4)},\\ \mathcal{N}^{(6)} &= \frac{1}{8}(1-p_{\rm d})(8+4p_{\rm d}+3p_{\rm d}^2)\mathcal{N}_0,\\ \mathcal{N}^{(7)} &= \mathcal{N}^{(6)}.\end{aligned} \tag{11}$$

From Eq. (11), with the same $\mathcal{N}_0$, the entanglement for the states $|\Psi^n\rangle$ in Eq. (5) does not decrease with n, namely,

$$\mathcal{N}^{(2)} = \mathcal{N}^{(3)} \leq \mathcal{N}^{(4)} = \mathcal{N}^{(5)} \leq \mathcal{N}^{(6)} = \mathcal{N}^{(7)}. \tag{12}$$

In other words, the entanglement of $|\Psi^n\rangle$ does not become more fragile when the size of system increases.

Next, we discuss the other form of pure states for an arbitrary n-qubit system

$$\begin{aligned}|\Phi^n\rangle &= \frac{{\rm e}^{{\rm i}\theta}}{2}(|0\rangle^{\otimes n}+|1\rangle^{\otimes n})\\ &\quad+\frac{{\rm e}^{-{\rm i}\theta}}{2}(|0\rangle|1\rangle^{\otimes(n-1)}+|1\rangle|0\rangle^{\otimes(n-1)}),\end{aligned} \tag{13}$$

where $\theta \in [0, \pi/2]$. These states are related to the states $|\Psi^n\rangle$ by an LU transformation as

$$|\Phi^n\rangle = H_1^{\otimes(n-1)} \otimes H_2 |\Psi^n\rangle, \tag{14}$$

with

$$H_1 = \frac{1}{\sqrt{2}}\begin{pmatrix}1 & 1\\ 1 & -1\end{pmatrix}, \quad H_2 = \frac{1}{\sqrt{2}}\begin{pmatrix}1 & 1\\ -1 & 1\end{pmatrix}, \tag{15}$$

which are both the Hadamard matrices. That is, $|\Phi^n\rangle$ are LU-equivalent to $|\Psi^n\rangle$. Therefore, these two special forms of states possess precisely the same amount and type of entanglement in absence of decoherence. Specifically, the bipartite entanglement of the initial states (13) can also be expressed as $\mathcal{N}_0 = \sin 2\theta$.

The partial transposed density matrix $\rho_{\Phi^n}^{T_A}(t)$ under the dephasing channel is given by

$$\begin{aligned}\rho_{\Phi^n}^{T_A}(t) &= \frac{1}{4}\sum_{i=0,1}\Big\{(|i\rangle\langle i|)^{\otimes n}+|i\rangle\langle i|\otimes(|1-i\rangle\langle 1-i|)^{\otimes(n-1)}\\ &\quad+\Big[|i\rangle\langle 1-i|\otimes(|1-i\rangle\langle i|)^{\otimes(n-1)}+(|i\rangle\langle 1-i|)^{\otimes n}\Big]s^{n/2}\\ &\quad+{\rm e}^{2{\rm i}\theta}\Big[|i\rangle\langle 1-i|\otimes(|1-i\rangle\langle 1-i|)^{\otimes(n-1)}s^{1/2}\\ &\quad+|i\rangle\langle i|\otimes(|i\rangle\langle 1-i|)^{\otimes(n-1)}s^{(n-1)/2}\Big]+{\rm h.c.}\Big\},\end{aligned} \tag{16}$$

here h.c. represents the hermitian conjugate of the previous terms. The matrix has only one negative eigenvalue which is determined by the following 4×4 matrix:

$$\rho^{T}(t) = \frac{1}{4}\begin{pmatrix}1 & {\rm e}^{2{\rm i}\theta}s^{(n-1)/2} & {\rm e}^{-2{\rm i}\theta}s^{1/2} & s^{n/2}\\ {\rm e}^{-2{\rm i}\theta}s^{(n-1)/2} & 1 & s^{n/2} & {\rm e}^{2{\rm i}\theta}s^{1/2}\\ {\rm e}^{2{\rm i}\theta}s^{1/2} & s^{n/2} & 1 & {\rm e}^{-2{\rm i}\theta}s^{(n-1)/2}\\ s^{n/2} & {\rm e}^{-2{\rm i}\theta}s^{1/2} & {\rm e}^{2{\rm i}\theta}s^{(n-1)/2} & 1\end{pmatrix}. \tag{17}$$

The negativities corresponding to the bipartition $q_1|Q_{n-1}$ for the states in Eq. (13) can be expressed as

$$\mathcal{N}^{(n)} = \max\left\{0, \frac{1}{2}\left[(1-p_{\rm d})^{n/2}+\sqrt{(4\mathcal{N}_0^2-2)(1-p_{\rm d})^{n/2}+(1-p_{\rm d})^{n-1}+1-p}-1\right]\right\}. \tag{18}$$

Contrary to the case of $|\Psi^n\rangle$, the negativities of $|\Phi^n\rangle$ do not increase with n according to Eq. (18), namely,

$$\mathcal{N}^{(n+1)} \leq \mathcal{N}^{(n)}. \tag{19}$$

It indicates that, unlike $|\Psi^n\rangle$, the entanglement of $|\Phi^n\rangle$ which can be transformed into $|\Psi^n\rangle$ by local operations, does not become more robust with the increase of n. For comparison, with $\theta = \pi/4$, we display in Fig. 1 the entanglement evolutions of $|\Psi^n\rangle$ with solid lines or dashed dot dot lines and $|\Phi^n\rangle$ with dashed lines for the systems with $n = 2, 3, \ldots, 7$, respectively (shown with gray, pink, blue, green, orange, black curves, respectively), under the local dephasing channel. From Fig. 1, one can see clearly that the entanglement evolutions of both the two forms of states change with n and so do the differences of entanglement evolutions between the two forms. Furthermore, it suggests that LU operations which do not change the entanglement properties of a state can enhance the robustness of an n-qubit system against decoherence.

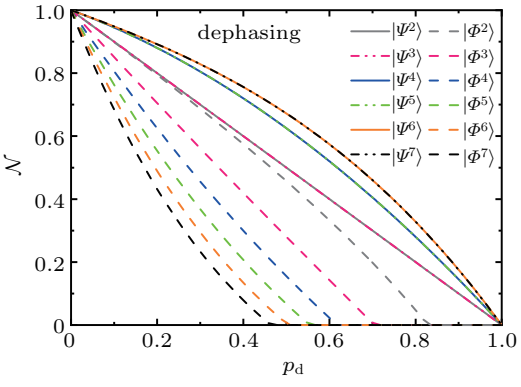


Fig. 1. Negativities of bipartition $q_1|Q_{n-1}$, as a function of $p_{\rm d}$, for the states $|\Psi^n\rangle$ (solid lines or dashed dot dot lines) and $|\Phi^n\rangle$ (dashed lines) with $\theta = \pi/4$ under the local dephasing. The systems with $n = 2, 3, \ldots, 7$ are shown with gray, pink, blue, green, orange, black curves, respectively.

3.2. Robustness of multiqubit pure states under the dephasing channel

In our previous work,[27] we found that the state $|\Psi^3\rangle$ in Eq. (5) is the most robust entangled state, and the state $|\Phi^3\rangle$ in

Eq. (13) is the most fragile entangled one under the dephasing channel. Now, we turn to the decoherence process of all n-qubit pure states under the dephasing channel with numerical calculation. The remaining negativity $\mathcal{N}$ of a state which is affected by the fixed decoherence noise is used as the quantifier of robustness. By taking a four-qubit system as an example, we sample 3×10^4 random four-qubit entangled pure states with the Haar measure[36] and compute their remaining entanglements with $p_{\rm d}$ taking the values $1/8$, $2/8$, $3/8$, and $4/8$, respectively. The corresponding remaining negativities $\mathcal{N}$ are plotted in Figs. 2(a)–2(d) with gray solid dots. In addition, according to Eq. (10) and Eq. (18), one can easily get the relation between $\mathcal{N}$ and $\mathcal{N}_0$ with the same values of $p_{\rm d}$ corresponding to the state $|\Psi^4\rangle$ in Eq. (5) and the state $|\Phi^4\rangle$ in Eq. (13). In Figs. 2(a)–2(d), the remaining negativities are depicted with red solid lines for state $|\Psi^4\rangle$ and olive dashed lines for state $|\Phi^4\rangle$.

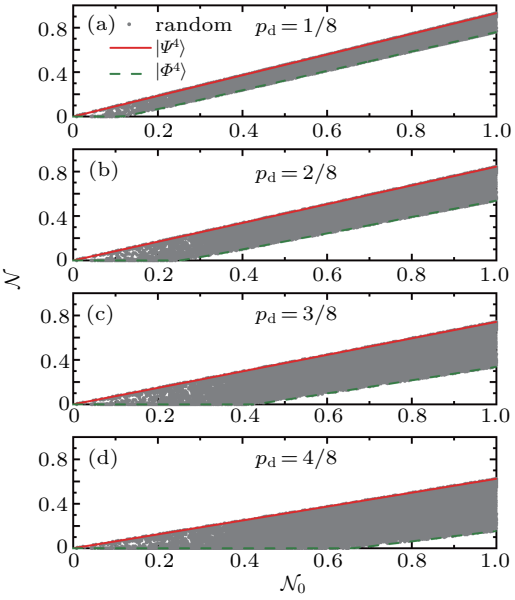


Fig. 2. The remaining negativities $\mathcal{N}$ *versus* the initial entanglement $\mathcal{N}_0$ for a four-qubit system in the 3×10^4 random sampled pure states (gray solid dots), special states $|\Psi^4\rangle$ (red solid lines) and $|\Phi^4\rangle$ (olive dashed lines) under the dephasing channel. We plot the remaining negativities characterizing robustness of the state when the dephasing noise $p_{\rm d}=1/8$, $2/8$, $3/8$, and $4/8$ in panels (a), (b), (c), and (d), respectively. The same behavior is displayed for all other noise parameters and for systems with $n=2,3,5,6$, and 7.

In Fig. 2, the remaining negativities $\mathcal{N}$ of 3×10^4 random four-qubit pure states display ribbon distributions. The red solid lines are the upper bounds; while the olive dashed lines are the lower bounds. In other words, state $|\Psi^4\rangle$ is the most robust entangled state, while state $|\Phi^4\rangle$ is the most fragile one for the four-qubit system during decoherence under the dephasing channel, although they are LU-equivalent with each other. The results imply that the suitable LU operations can enhance the robustness of entanglement to the max. We also explored the dephasing process of another multiqubit pure state with $n=2,5,6$, and 7, and obtain the same result. Therefore, we suppose that the conclusion is universal for n-qubit entanglement corresponding to the bipartition $q_1|Q_{n-1}$.

4. Robustness of entanglement under bit flip channel

4.1. Evolution of special states under bit flip channel

The bit flip channel is the same as the dephasing channel under the local rotational transformation. It flips the state of a qubit between $|0\rangle$ and $|1\rangle$ with a certain probability and each qubit is affected by the noise correspondingly. The states $|\Phi^n\rangle$ in Eq. (13) and $|\Psi^n\rangle$ in Eq. (5), which can be transformed into each other by local operations and manifest the most significant difference in robustness under the dephasing channel, are worth to be investigated further for this channel. Similarly, we also take the example of the pure states $|\Phi^4\rangle$ and $|\Psi^4\rangle$ to calculate the negativities under the bit flip channel. We need to write the nonzero elements of the partial transposed density matrix $\rho^{T_A}_{\Phi^4}(t)$ and $\rho^{T_A}_{\Psi^4}(t)$ during the evolution, which are given in Appendix A. Here the negativities expressions of $|\Phi^n\rangle$ with $n=2,3,\ldots,7$, are straightforwardly provided as follows:

$$\begin{aligned}
\mathcal{N}^{(2)} &= (1-p_{\rm bf})^2\mathcal{N}_0,\\
\mathcal{N}^{(3)} &= \mathcal{N}^{(2)},\\
\mathcal{N}^{(4)} &= \frac{1}{2}(1-p_{\rm bf})^2\left(2+2p_{\rm bf}-p_{\rm bf}^2\right)\mathcal{N}_0,\\
\mathcal{N}^{(5)} &= \mathcal{N}^{(4)},\\
\mathcal{N}^{(6)} &= \frac{1}{8}(1-p_{\rm bf})^2\left(8+8p_{\rm bf}+8p_{\rm bf}^2-12p_{\rm bf}^3+3p_{\rm bf}^4\right)\mathcal{N}_0,\\
\mathcal{N}^{(7)} &= \mathcal{N}^{(6)}.
\end{aligned}\tag{20}$$

The negativities between the bipartition $q_1|Q_{n-1}$ for the states $|\Psi^n\rangle$ under the bit flip channel are given by

$$\mathcal{N}^{(n)}=\max\left\{0,\ \frac{1}{2}\Big[-1+(1-p_{\rm bf})^n+\sqrt{4\mathcal{N}_0^2(1-p_{\rm bf})^n+\left[1-p_{\rm bf}-(1-p_{\rm bf})^n\right]^2}\Big]\right\}.\tag{21}$$

With the same $\mathcal{N}_0$, the entanglement evolutions of $|\Phi^n\rangle$ and $|\Psi^n\rangle$ for the systems with $n=2,3,\ldots,7$ under the bit flip channel have the same features as Eq. (12) and Eq. (19), respectively. When $\theta=\pi/4$, the curves of negativity *versus* $p_{\rm bf}$ are plotted for $|\Phi^n\rangle$ with solid lines or dashed dot dot lines and for $|\Psi^n\rangle$ with dashed lines in Fig. 3 for the systems with $n=2,3,\ldots,7$, respectively (shown with gray, pink, blue, green, orange, black curves, respectively). From the figure, one can see obviously that there are differences in the evolution of entanglement, although the corresponding two forms of states are LU-equivalent, and the difference increases with qubits n. Furthermore, the states $|\Phi^n\rangle$ are more robust than the states $|\Psi^n\rangle$ under the bit flip channel.

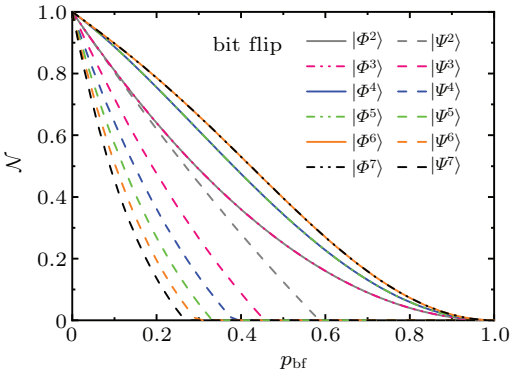


Fig. 3. Negativities of bipartition $q_1|Q_{n-1}$, as a function of $p_{\rm bf}$, for the states $|\Phi^n\rangle$ (solid lines or dashed dot dot lines) and $|\Psi^n\rangle$ (dashed lines) with $\theta = \pi/4$ under the bit flip channel. The systems with $n = 2,3,\ldots,7$ are shown with gray, pink, blue, green, orange, black curves, respectively.

4.2. Robustness of multiqubit pure states under the bit flip channel

The decoherence process of all multiqubit pure states under the bit flip channel is also explored similar to the case of the dephasing channel. We plot the remaining negativities $\mathcal{N}$ for the state $|\Phi^4\rangle$ in Eq. (13), the state $|\Psi^4\rangle$ in Eq. (5), and random sampled states when the degree of bit flip $p_{\rm bf} = 1/8$, $2/8$, $3/8$, and $4/8$ with olive dashed lines, red solid lines, and gray solid dots in Figs. 4(a)–4(d), respectively.

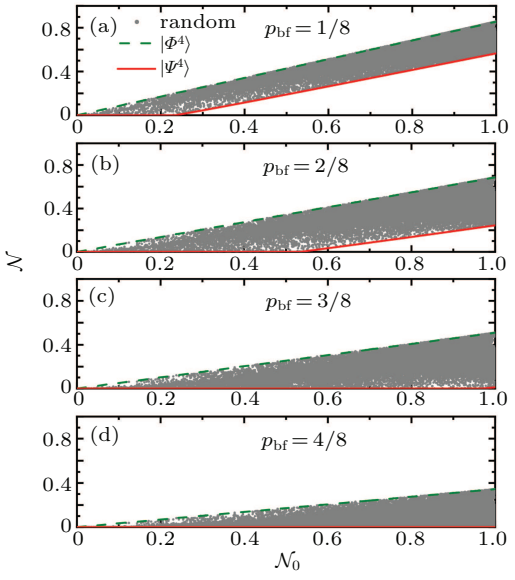


Fig. 4. The remaining negativities $\mathcal{N}$ *versus* the initial entanglement $\mathcal{N}_0$ for a four-qubit system in the 3×10^4 random sampled pure states (gray solid dots), special states $|\Phi^4\rangle$ (red solid lines) and $|\Psi^4\rangle$ (olive dashed lines) under the bit flip channel. We plot the remaining negativities characterizing robustness of the state when the bit flip noise $p_{\rm bf} = 1/8$, $2/8$, $3/8$, and $4/8$ in panels (a), (b), (c), and (d), respectively. The same behavior is displayed for all other noise parameters and for systems with $n = 2,3,5,6$, and 7.

From the figure, one can see that there is a ribbon distribution for $\mathcal{N}$ of 3×10^4 random four-qubit pure states. Since the same unitary operation also connects the bit flip channel with the dephasing channel, the state $|\Phi^4\rangle$ is the most robust entangled state, while the state $|\Psi^4\rangle$ is the most fragile one under the bit flip channel. For the cases of $n = 2,3,5,6,7$, we have the same results. We suppose that the conclusion is universal for n-qubit entanglement corresponding to the bipartition $q_1|Q_{n-1}$.

5. Conclusion

In summary, we have investigated the robustness of entanglement for a multiqubit system under the dephasing and the bit flip channels. We explore the entanglement evolutions of two forms of special n-qubit states $|\Psi^n\rangle$ and $|\Phi^n\rangle$ which are LU-equivalent to each other and therefore posses precisely the same amount and type of entanglement. For the dephasing channel, with $n = 2,3,\ldots,7$, the robustness of the states $|\Psi^n\rangle$ does not decrease with n, while for the states $|\Phi^n\rangle$, the robustness does not increase with the size of system. The larger number of qubits a system has, the greater distinction the entanglement evolution of those states manifests. Moreover, by comparing the remaining negativities of the special quantum states with that of random pure states, we find that the states $|\Psi^n\rangle$ are the most robust states and the states $|\Phi^n\rangle$ are the most fragile ones.

Similarly, for bit flip channel, the states $|\Phi^n\rangle$ and $|\Psi^n\rangle$ also exhibit the most significant difference in robustness, but, contrary to the case of the dephasing channel, the states $|\Phi^n\rangle$ are the most robust states, while the states $|\Psi^n\rangle$ are the most fragile ones. Remarkably, our results suggest that the robustness of an arbitrary n-qubit system under decoherence can be greatly enhanced by LU operations. It might provide a possible way in protecting the robust n-qubit states against decoherence through appropriate LU operations.

Appendix A: Special states $|\Phi^4\rangle$ and $|\Psi^4\rangle$ under bit flip channel

The nonzero elements of the partial transposed density matrix $\rho^{T_A}_{\Phi^4}(t)$ of the state $|\Phi^4\rangle$ in Eq. (13) under the influence of bit flip channel can read as follows:

$$\rho_{mn}(t) = \frac{1}{16}\left(1+3s^2\right) \tag{A1}$$

with $m,n = 1,16$ and $m,n = 8,9$;

$$\rho_{mn}(t) = \frac{1}{16}\left(1-s^2\right) \tag{A2}$$

with $m = 2,3,\ldots,15, m \neq 8,9; n = m, 17-m$; and

$$\rho_{mn}(t) = \rho^*_{nm}(t) = \frac{\cos 2\theta}{16} + \frac{3\,\mathrm{e}^{2\mathrm{i}\theta}s^2 + \mathrm{i}\sin 2\theta s^4}{16}, \tag{A3}$$

where $m = 1, n = 8$; $m = 8, n = 16$; $m = 9, n = 1$, and $m = 16, n = 9$, and

$$\rho_{mn}(t) = \rho^*_{nm}(t) = \frac{\cos 2\theta}{16} - \frac{\mathrm{e}^{-2\mathrm{i}\theta}s^2 + \mathrm{i}\sin 2\theta s^4}{16}, \tag{A4}$$

where $m = 2,3,\ldots,15$, $m \neq 8,9$, and corresponding $n = 7$, 6, 12, 4, 14, 15, 2, 3, 13, 5, 11, and 10, respectively.

The nonzero elements of the partial transposed density matrix $\rho_{\Psi^4}^{\mathrm{T}_A}(t)$ of the state $|\Psi^4\rangle$ in Eq. (5) under the bit flip channel can read as follows:

$$\rho_{mn}(t)=\begin{cases}\dfrac{1}{16}\left(1-s^2\right)\left(1+\cos 2\theta s+s^2\right),\\ \quad \text{with}\ \ m,n=1,4,6,7;\\ \dfrac{1}{16}\left[1+\cos 2\theta\left(s+s^3\right)+s^4\right],\\ \quad \text{with}\ \ m,n=2,3,5,8;\\ \dfrac{1}{16}\left[1-\cos 2\theta\left(s+s^3\right)+s^4\right],\\ \quad \text{with}\ \ m,n=9,12,14,15;\\ \dfrac{1}{16}\left(1-s^2\right)\left(1-\cos 2\theta s+s^2\right),\\ \quad \text{with}\ \ m,n=10,11,13,16;\end{cases} \tag{A5}$$

$$\begin{aligned}\rho_{mn}(t)&=\rho_{nm}^{*}(t)\\ &=\begin{cases}\mathrm{i}\dfrac{\cos\theta\sin\theta}{8}\left(s+s^3\right),\\ \text{with}\ \ m=1,4,6,7;\ n=10,11,13,16,\\ \mathrm{i}\dfrac{\cos\theta\sin\theta}{8}\left(s-s^3\right),\\ \text{with}\ \ m=2,3,5,8;\ n=9,12,14,15.\end{cases}\end{aligned} \tag{A6}$$

References

[1] Nielsen M A, Chuang I L 2010 *Quantum Computation and Quantum Information* (Cambridge: Cambridge University Press)
[2] Horodecki R, Horodecki P, Horodecki M and Horodecki K 2009 *Rev. Mod. Phys.* **81** 865
[3] Bennett C H and Divincenzo D P 2000 *Nature* **404** 247
[4] Raussendorf R and Briegel H J 2001 *Phys. Rev. Lett.* **86** 5188
[5] Bennett C H, Brassard G, Crépeau C, Jozsa R, Peres A and Wootters W K 1993 *Phys. Rev. Lett.* **70** 1895
[6] Hu M L 2012 *Ann. Phys.* **327** 2332
[7] Ekert A K 1991 *Phys. Rev. Lett.* **67** 661
[8] Bennett C H, Brassard G and Mermin N D 1992 *Phys. Rev. Lett.* **68** 557
[9] Deng F G and Long G L 2003 *Phys. Rev. A* **68** 042315
[10] Sheng Y B and Zhou L 2017 *Sci. Bull.* **62** 1025
[11] Aolita L, Melo F de and Davidovich L 2015 *Rep. Prog. Phys.* **78** 042001
[12] Wang D, Shi W N, Hoehn Ross D, Ming F, Sun W Y, Kais S and Ye L 2018 *Ann. Phys.* **530** 1800080
[13] Chen M N, Wang D and Ye L 2019 *Phys. Lett. A* **383** 977
[14] Yu T and Eberly J H 2004 *Phys. Rev. Lett.* **93** 140404
[15] Yu T and Eberly J H 2009 *Science* **323** 598
[16] Roszak K, Horodecki P and Horodecki R 2010 *Phys. Rev. A* **81** 042308
[17] Almeida M P, de Melo F, Meyll H M, Salles A, Walborn S P, Ribeiro P H S and Davidovich L 2007 *Science* **316** 579
[18] Yönaç M, Yu T and Eberly J H 2006 *J. Phys. B: At. Mol. Opt. Phys.* **39** S621
[19] Yönaç M, Yu T and Eberly J H 2007 *J. Phys. B: At. Mol. Opt. Phys.* **40** S45
[20] Kim K I, Zhao B K and S Li H M 2014 *Commun. Theor. Phys.* **62** 667
[21] Li H M and Su X M 2019 *Eur. Phys. J. D* **73** 56
[22] Gühne O, Bodoky F and Blaauboer M 2008 *Phys. Rev. A* **78** 060301
[23] Borras A, Majtey A P, Plastino A R, Casas M and Plastino A 2009 *Phys. Rev. A* **79** 022108
[24] Ali M and Gühne O 2014 *J. Phys. B: At. Mol. Opt. Phys.* **47** 055503
[25] Zhao B K and S Deng F G 2010 *Phys. Rev. A* **82** 014301
[26] Zhang F L, Jiang Y and Liang M L 2013 *Ann. Phys.* **333** 136
[27] Li H M and S Zhao B K 2018 *Ann. Phys.* **530** 1800053
[28] Man Z X, Xia Y J and An N B 2008 *Phys. Rev. A* **78** 064301
[29] Aolita L, Chaves R, Cavalcanti D, Acin A and S Davidovich L 2008 *Phys. Rev. Lett.* **100** 080501
[30] Salles A, de Melo F, Almeida M P, Hor-Meyll M, Walborn S P, Souto Ribeiro P H and S Davidovich L 2008 *Phys. Rev. A* **78** 022322
[31] Kraus K 1983 *States, Effect, and Operation: Fundamental Notions in Quantum Theory* (Berlin: Springer-Verlag)
[32] Życzkowski K, Horodecki P, Sanpera A and Lewenstein M 1998 *Phys. Rev. A* **58** 883
[33] Peres A 1996 *Phys. Rev. Lett.* **77** 1413
[34] Vidal G and Werner R F 2002 *Phys. Rev. A* **65** 032314
[35] Lee S, Chi D P, Oh S D and Kim J 2003 *Phys. Rev. A* **68** 062304
[36] Życzkowski K and Kuś M 1994 *J. Phys. A: Math. Gen.* **27** 4235